

## STUDY OF THE COMBUSTION MECHANISM OF OIL SHALE SEMI-COKE WITH RICE STRAW BASED ON GAUSSIAN MULTI-PEAK FITTING AND PEAK-TO-PEAK METHODS

WANG QING\*, WANG XUDONG, LIU HONGPENG,  
JIA CHUNXIA

Engineering Research Centre of Oil Shale Comprehensive Utilization  
Ministry of Education, Northeast Dianli University  
Jilin 132012, Jilin, China

**Abstract.** *In this research, a series of experiments on combustion of Huadian oil shale semi-coke and rice straw as well as their mixture were conducted at different heating rates (10, 20, 50 and 80 °C/min) under atmospheric pressure, using a Perkin Elmer thermogravimetric analyzer. Combustion characteristics were investigated at different proportions of materials (L1, L2, L3, L4 and L5) and at different heating rates. The results revealed that the point of ignition and burnout shifted to lower temperature with increasing rice straw proportion in the mixture. In the combustion process, the interaction between the mixture components mainly occurred in the temperature range of 400 to 600 °C. It was found that in this stage the reaction of bimodal components of semi-coke and rice straw took place. Besides, using the Gaussian multi-peak fitting method it was established that the derivative mass loss (DTG) curves displayed an overlapping peak, which consisted of three sub-peaks corresponding to the components of the blend. Moreover, based on the three sub-peaks, kinetic parameters and feature values were found employing the peak-to-peak method. The results showed that the reaction order of various sub-peaks for samples L1, L2, L3 and L4 was 1.17 to 2.27. The activation energies of sub-peaks were determined to be 21.89–99.79 KJ/mol throughout the analysis of the combustion mechanism. It was concluded that the model can be applied to determining combustion characteristics.*

**Keywords:** *oil shale, semi-coke, rice straw, kinetics, Gaussian multi-peak fitting method, peak-to-peak method.*

---

\* Corresponding author: e-mail [rlx888@126.com](mailto:rlx888@126.com)

## 1. Introduction

There are several accepted definitions of oil shale. According to one of them oil shale is a “kind of energy resource which is widely distributed around the world.” Oil shale semi-coke, obtained in abundance from oil shale retorting, is a useable waste product [1, 2]. Semi-coke has been considered to have a detrimental impact on the environment due to the trace metals and PAHs (polycyclic aromatic hydrocarbons) present [3, 4]. Nowadays, the bottleneck in the development of the oil shale industry is how to deal with these solid residues efficiently. This issue has been extensively addressed by several researchers. Martins et al. [5] proposed that semi-coke can be mostly burnt in fluidized bed boilers. Wang et al. [6, 7] thought that semi-coke can be utilized when it was moderately mixed with oil shale. Sun et al. [8] investigated the combustion characteristics of a mixture of bituminous coal and semi-coke. Wang et al. [9] found that combustion characteristics can be improved when cornstalk was mixed with oil shale semi-coke. Not only the utilization of semi-coke can be improved to a certain extent, but also its impact on the environment is reduced.

At present, biomass as a renewable energy source has become an increasingly attractive fuel to limit the generation of pollutants. Among other solid fuels, it is the fourth largest energy resource [10]. Biomass can either be burned directly, or converted into other energy products such as oil. Furthermore, biomass can be utilized together with coal. De et al. [11] found that the firing of biomass with coal was an effective way to decrease CO<sub>2</sub> emission from a power plant. Yang et al. [12] discovered that alkali metals, such as KOH, NaCl, NaOH and KCl, can be sharply reduced to protect the environment from pollution during co-combustion of biomass and coal. Munir et al. [13] investigated features of the co-firing of biomass and coal and found that this might reduce air pollution, such as NO<sub>x</sub> emissions, and improve combustion efficiency.

In recent years, some thermal methods have been extensively used to study the combustion kinetics of solid fuels. These methods are mainly used to analyze the combustion process on the basis of mass loss (TG) and derivative mass loss (DTG) curves. However, they do not take into account the overlapping peak. In this work, the overlapping peak reflects the reaction of bimodal components of semi-coke and rice straw, whose peaks overlap in the combustion process and cannot be distinguished separately on the combustion curves. The study of the overlapping peak, in whose region the reaction of some blend components occurs, is useful to understand the combustion mechanism. The investigation of the overlapping peak is conducted to fill in the gaps of previous studies, which neglected or oversimplified its processing. In this work, there is an overlapping peak resulting from the merger of sub-peaks in the major stage of combustion (400–600 °C). Based on DTG curves, three sub-peaks can be separated from the overlapping peak, using the Gaussian multi-peak fitting method, which is widely applied in

such cases. In order to study the combustion kinetics of components behind the three sub-peaks, a peak-to-peak method is used. Several researches have been carried out in different fields to investigate combustion kinetics. For example, Soboleva et al. [14] and Romanenko et al. [15, 16] proposed mathematical methods of separation to be employed in analytical chemistry. When analyzing combustion kinetics, Wang et al. [17, 18] and Huang et al. [19] were of the opinion that during pyrolysis biomass was separated into three components. Li et al. [20, 21] and Ma et al. [22] believed that the multi-peak fitting method was suitable for separation of the overlapping peak of DTG curves, which can be used to analyze the combustion kinetics of biomass.

So far, there is no report about the co-combustion of oil shale semi-coke and rice straw. In this work, Gaussian multi-peak fitting and peak-to-peak methods are applied to studying the combustion of the blend of oil shale semi-coke and rice straw. The sub-peaks, which are separated from the overlapping peak, are analyzed using the peak-to-peak method. The procedures presented and methods used in this work could be applicable to a much wider range of similar kinetic problems. The investigation of the co-combustion mechanism of oil shale semi-coke and rice straw is valuable from a viewpoint of future applications of the process.

## 2. Thermogravimetric experimental

### 2.1. Materials

In this research, oil shale semi-coke (SC) was obtained from Huadian oil shale retort factory located in Jilin Province, China. Rice straw (RS) was also from Jilin Province. Samples with different blending ratios were labeled as L1, L2, L3, L4, and L5. The particles were ground and sieved to the size of 0–0.2 mm according to the ASTM standards. The blending ratio (SC/RS) is given in Table 1. The data on proximate and ultimate analyses of SC and RS blends are presented in Table 2.

**Table 1. Sample labels and the blending ratio**

Sample label	L1	L2	L3	L4	L5
Blending ratio, SC/RS	10:0	9:1	8:2	7:3	0:10

**Table 2. Proximate and ultimate analyses of oil shale semi-coke and rice straw blends**

Component	Proximate, %				Q <sub>ne,ar</sub> , kJ/kg	Ultimate, %				
	M <sub>ad</sub>	V <sub>ad</sub>	A <sub>ad</sub>	FC <sub>ad</sub>		C <sub>ad</sub>	H <sub>ad</sub>	O <sub>ad</sub>	N <sub>ad</sub>	S <sub>ad</sub>
SC	0.89	10.44	82.62	6.09	3868.29	11.29	0.35	4.21	0.11	0.53
RS	7.05	66.81	9.56	16.58	14468.90	36.55	5.49	40.01	0.78	0.56

## 2.2. Experimental facilities and method

Combustion experiments were conducted by a Perkin Elmer Pyris 1 Thermal Analyzer under atmospheric pressure. The average mass of the sample was about 6 mg, the air flow was kept constant at 80 L/min. Experimental samples were placed in a sample pan and the corresponding experiments were performed at different heating rates (10, 20, 50 and 80 °C/min) within the temperature range of 40–900 °C. All experiments were repeated at least twice to ensure the repeatability and accuracy of test data.

## 2.3. Results and discussion

The mass loss (TG) and derivative mass loss (DTG) curves obtained from thermogravimetric experiments carried out at different heating rates (10, 20, 50 and 80 °C/min) are shown in Figures 1–4, respectively. Figures 1 and 2 show TG/DTG data of sample L3 at different heating rates (10, 20, 50 and 80 °C/min). It may be observed that higher heating rates are accompanied by higher reaction temperatures and higher reaction rates. The peak temperature shifts to the higher temperature with increasing heating rate. The higher the heating rate is, the higher the temperature of burnout is. The lateral shifts in TG/DTG curves are shown in Figures 1 and 2. This result is due to the acceleration of variations in the rate of heat transfer with increasing heating rate and the decrease of exposure time at a particular temperature at higher heating rates [23, 24], which leads to the increase of temperature. It was also found that the maximum rate of burning increased at higher heating rates. With decreasing heating rate, however, the burning of particles was delayed, which means the need to improve the burnout of sample L3. This may be explained by that the temperature gradient inside and outside the particles is lower at the lower heating rate, which somewhat increases the release of the volatile matter [25].

A typical variation of TG/DTG data with temperature at a heating rate of 20 °C/min is given in Figures 3–4. It can clearly be seen from these figures that with increasing proportion of rice straw in the blend the mass loss region on TG curves increases and the width and temperature of the peak on DTG curves of sample increase. This may be attributed to the improvement of combustion when oil shale semi-coke is mixed with rice straw.

In this work, with increasing proportion of rice straw in the blend, combustion curves are divided into different regions. So, it is established that the TG/DTG curves of combustion have four distinct regions. First, the release of the volatile matter of rice straw took place in the first stage (200–400 °C). Then, the combustion of the easy-to-pyrolyze volatile matter of oil shale semi-coke occurred in the second stage (400–500 °C). Furthermore, the combustion of the fixed carbon of rice straw and the difficult-to-pyrolyze volatile matter in the oil shale semi-coke happened in the third stage (500–600 °C). Finally, the combustion of the fixed carbon in the oil shale semi-coke and other difficult-to-decompose materials took place in the fourth stage (600–900 °C).

Above all, combustion features of oil shale semi-coke can be improved, the combustion becomes more stable after mixing semi-coke with rice straw. The combustion parameters for samples L1–L5, such as ignition temperature, maximum burning rate, peak temperature and burnout temperature, are summarized in Table 3. The ignition temperature  $T_i$  is found using the method of TG/DTG extrapolation [6, 26]. In Table 3,  $(dw/dt)_{max}^i$  is the maximum burning rate and  $T_{max}^i$  is the peak temperature. The burnout temperature  $T_h$  is defined as the temperature on the DTG curve at which the combustion or exothermic reactions are completed [27, 28]. The corresponding sketch map of  $T_i$  and  $T_h$  for sample L3 at a heating rate of 20 °C/min is shown in Figure 5.

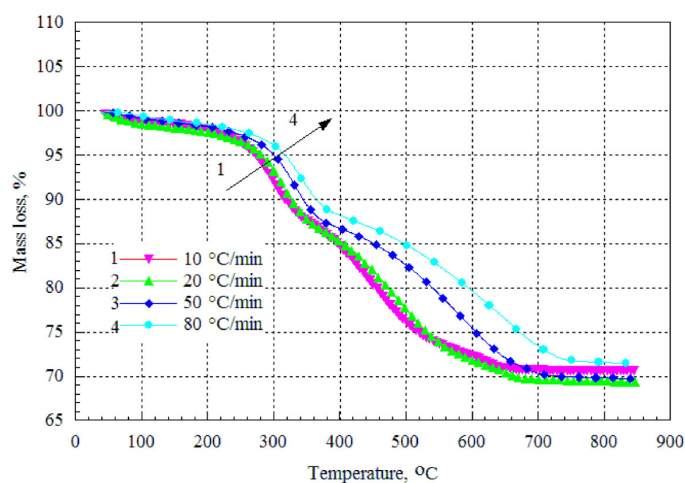


Fig. 1. TG curves of sample L3 at various heating rates.

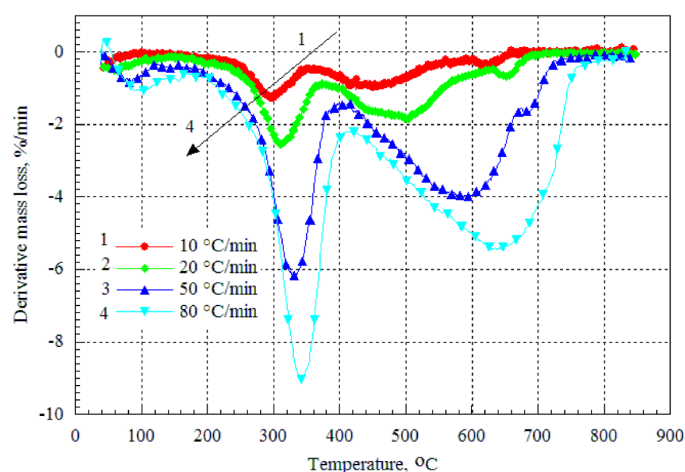


Fig. 2. DTG curves of sample L3 at various heating rates.

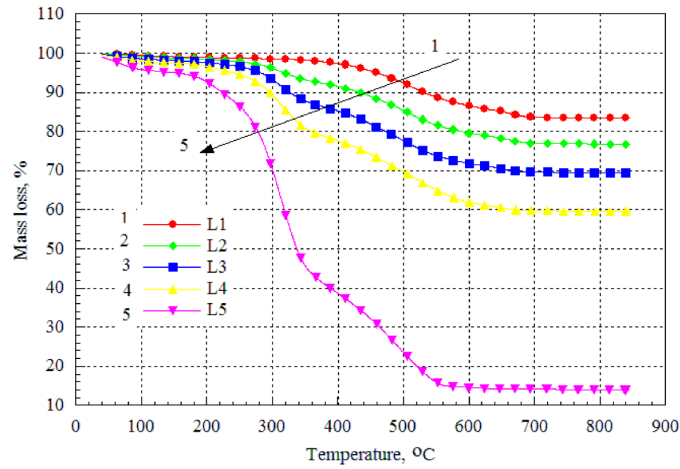


Fig. 3. TG curves of combustion of SC/RS mixtures at a heating rate of 20 °C/min.

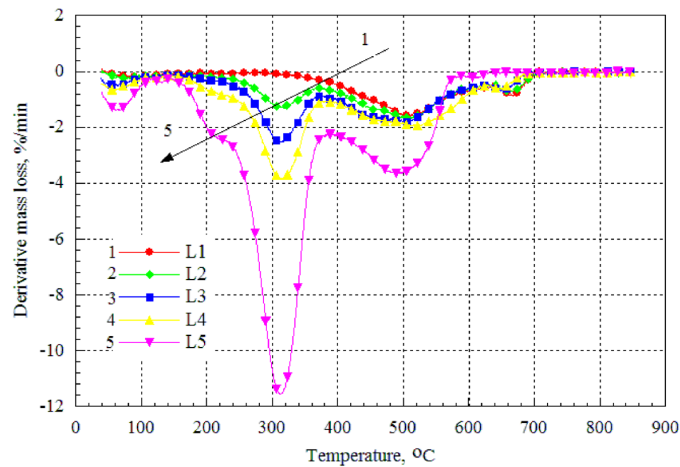


Fig. 4. DTG curves of combustion of SC/RS mixtures at a heating rate of 20 °C/min.

**Table 3. Combustion parameters for different samples**

Sample	Heating rate, °C/min	$T_i$ , °C	$T_h$ , °C	$T_{max}^1$ , °C	$(dw/dt)_{max}^1$ , %/min	$T_{max}^2$ , °C	$(dw/dt)_{max}^2$ , %/min	$T_{max}^3$ , °C	$(dw/dt)_{max}^3$ , %/min
L1	20	420.3	697.1	528.2	1.51	667.9	0.88	702.3	0.14
L2	20	290.5	695.3	312.6	1.30	503.5	1.69	661.6	0.75
L3	10	275.7	660.9	292.2	1.24	450.8	0.98	633.1	0.45
	20	282.5	688.4	309.7	2.54	504.0	1.84	652.9	0.69
	50	305.4	730.9	328.5	6.20	579.3	4.00	678.9	1.69
L4	80	320.1	775.5	342.1	9.04	638.9	5.44	803.3	0.26
	20	276.6	670.8	314.3	3.06	532.4	1.90	646.9	0.65
L5	20	240.4	566.5	312.7	11.56	492.2	3.65	608.4	0.25

$T_i$  – ignition temperature;  $T_h$  – burnout temperature;  $(dw/dt)_{max}^i$  – the maximum burning rate in stage  $i$ ,  $i = 1, 2, 3$ ;  $T_{max}^i$  – the peak temperature in stage  $i$ ,  $i = 1, 2, 3$ .

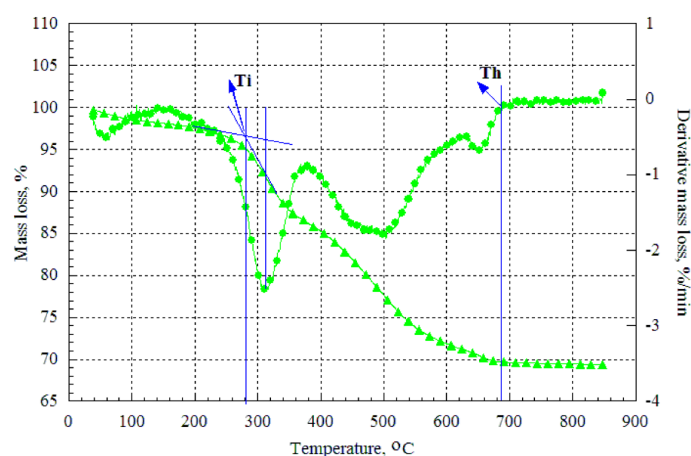


Fig. 5. Sketch map of  $T_i$  and  $T_h$  for sample L3 at a heating rate of 20 °C/min.

### 3. Theory

#### 3.1. Selection of combustion reaction region

Wang et al. [13] studied the combustion process of oil shale semi-coke and cornstalk based on TG/DTG curves. Their experimental results showed that the second (400–500 °C) and third (500–600 °C) stages were merged in one stage in the combustion process. It was also established that reactions occurring in this stage were more complex than those taking place in the others. However, the stage was not thoroughly analyzed by Wang et al.

In this research, the same phenomenon is discovered from DTG curves. So, the second (400–500 °C) and third (500–600 °C) stages of the reaction are merged in the 400–600 °C stage. It may be concluded that the interaction between blend components in the co-firing process occurred predominantly in the 400–600 °C range. Also, in this stage, some additional peaks or peak shoulders appeared. The reason is that several sub-peaks overlap at this stage. Hence, it is necessary to separate and study the overlapping peak from this stage.

#### 3.2. Gaussian multi-peak fitting method and separation of the overlapping peak

The Gaussian multi-peak fitting method, which increases the signal resolution by a numerical calculation and mathematical algorithm based on an appropriate function as a peak fitting function, is widely applied in various types of model analysis. The method is especially useful to separate and analyze the overlapping peak [21, 22]. Therefore, in the present work, the overlapping peak is first separated into a series of sub-peaks by using this method. Then, the Gaussian multi-peak fitting method is employed to calculate kinetic parameters, which can be expressed as follows [29]:

$$\begin{aligned}
y &= y_0 + \sum_{i=1}^n \frac{A_n}{\omega_n \sqrt{\pi/2}} \exp \left[ -2 \frac{x - x_{c_n}}{\omega_n^2} \right] \\
&= y_0 + \frac{A_1}{\omega_1 \sqrt{\pi/2}} \exp \left[ -2 \frac{x - x_{c_1}}{\omega_1^2} \right] + \frac{A_2}{\omega_2 \sqrt{\pi/2}} \exp \left[ -2 \frac{x - x_{c_2}}{\omega_2^2} \right] \\
&\quad + \frac{A_3}{\omega_3 \sqrt{\pi/2}} \exp \left[ -2 \frac{x - x_{c_3}}{\omega_3^2} \right] + \dots + \frac{A_n}{\omega_n \sqrt{\pi/2}} \exp \left[ -2 \frac{x - x_{c_n}}{\omega_n^2} \right], \quad (1)
\end{aligned}$$

where  $y_0$  is the baseline,  $A_n$  is the area of different sub-peaks,  $\omega_n$  is the FWHM (full width at half maximum) of different sub-peaks and  $x_n$  is the position of different sub-peaks,  $n \geq 1$ .

Based on the above equations, qualitative analysis of samples L1, L2, L3 and L4 is conducted at a heating rate of 20 °C/min in the major stage, 400–600 °C. According to this major stage of the combustion reaction, the relationship of  $da/dT$  vs  $T$  is plotted. Next, the position of the overlapping peak is determined. Finally, the overlapping peak is separated into three sub-peaks from the curves of  $da/dT$  vs  $T$ , using the Gaussian multi-peak fitting method. The results are shown in Figures 6–9.

### 3.3. Kinetics parameters of various sub-peaks

In general, the combustion of sample is regarded as a non-isothermal and non-homogeneous process. The process is analyzed using thermogravimetric (TG–DTG) data and a kinetic equation, The kinetic equation is always employed to simulate this process. Co-combustion, however, represents a

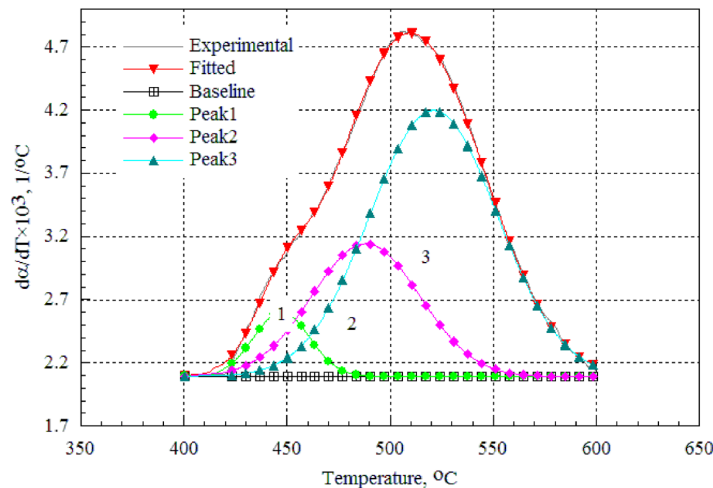


Fig. 6. Separation of the overlapping peak of sample L1 obtained at 20 °C/min.

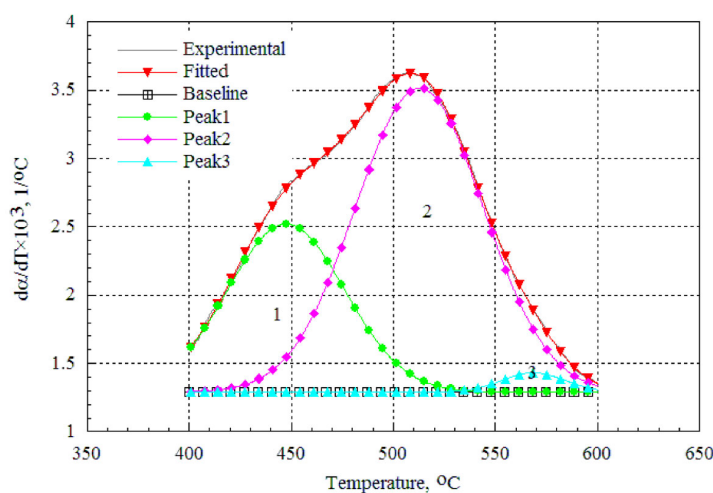


Fig. 7. Separation of the overlapping peak of sample L2 obtained at 20 °C/min.

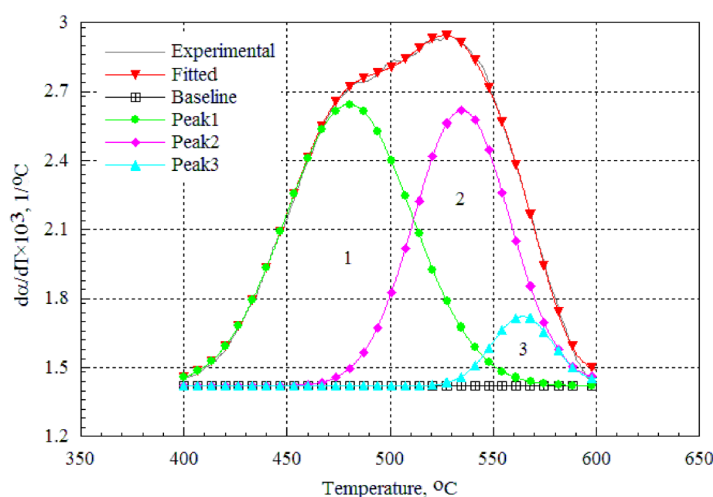


Fig. 8. Separation of the overlapping peak of sample L3 obtained at 20 °C/min.

multi-step decomposition process which is difficult to solve by a formal kinetic equation. The existing mechanism function cannot cover the entire multi-step process. Based on the formal kinetic equation, the peak-to-peak method is employed to analyze kinetic parameters of various sub-peaks appearing during co-combustion. The method uses feature values to accurately describe this multi-step process. The derivation step is described according to [22, 30].

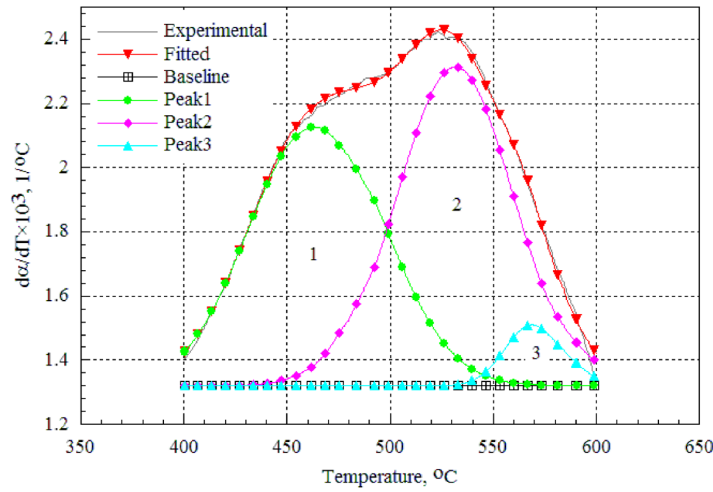


Fig. 9. Separation of the overlapping peak of sample L4 obtained at 20 °C/min.

The formal kinetic equation is expressed as follows:

$$\frac{d\alpha}{dT} = \frac{A}{\beta} \exp\left(-\frac{E}{RT}\right) f(\alpha), \quad (2)$$

where  $\alpha$  is the extent of conversion;  $\beta$  is the heating rate, °C/min;  $A$  is the frequency factor, 1/s;  $E$  is the activation energy, kJ/mol;  $R$  is the gas constant,  $8.314 \times 10^{-3}$  kJ/(mol/K);  $T$  is the absolute temperature, K; and  $f(\alpha)$  is a function.

According to the solid-state combustion process, a combustion reaction may be presented as a function:

$$f(\alpha) = (1 - \alpha)^n. \quad (3)$$

Substituting Equation (3) for Equation (2), the expression can be modified as follows:

$$\frac{d\alpha}{dT} = \frac{\beta}{A} \exp\left(-\frac{E}{RT}\right) (1 - \alpha)^n. \quad (4)$$

For a non-isothermal kinetic experiment, Equation (4) can be calculated by the following partial derivative:

$$\begin{aligned} dT &= \beta dt \neq 0 \\ \left(\frac{d\alpha}{dT}\right)' &= \left[\frac{\beta}{A} \exp\left(-\frac{E}{RT}\right) (1 - \alpha)^n\right]' \Rightarrow \frac{d^2\alpha}{dT^2} \\ &= \frac{\beta}{A} \exp\left(-\frac{E}{RT}\right) \frac{E}{RT^2} (1 - \alpha)^n - \frac{\beta}{A} \exp\left(-\frac{E}{RT}\right) n(1 - \alpha)^{n-1} \frac{d\alpha}{dT}. \end{aligned} \quad (5)$$

Based on the Gaussian multi-peak fitting method, the relationship of  $d\alpha/dT$  vs  $T$  corresponding to feature values can be obtained:

$$\frac{d\alpha}{dT_p} = \left(\frac{d\alpha}{dT}\right)_{\max} \Rightarrow \left(\frac{d\alpha}{dT_p}\right)' = \frac{d^2\alpha}{dT_p^2} = 0, \quad (6)$$

where  $T_p$  is the temperature of peak and  $(d\alpha/dT)_{\max}$  is the maximum value.

When  $T$  is equal to  $T_p$ , Equation (7) can be defined as follows:

$$E = nRT_p^2 \left(\frac{d\alpha}{dT}\right) (1 - \alpha_p)^{-1}, \quad (7)$$

where  $n$  is the reaction order and  $\alpha_p$  is the conversion corresponding to the temperature of peak.

Obviously, Equation (6) is determined according to the definition of half peak height:

$$\frac{1}{2} \left(\frac{d\alpha}{dT}\right)_p = \left(\frac{d\alpha}{dT}\right)_i = \frac{A}{\beta} \exp\left(-\frac{E}{RT_i}\right) (1 - \alpha_i)^n \quad (8)$$

$$T = T_p, T_i = T_p + \Delta T, \frac{\Delta T}{T_p} \ll 1,$$

where  $T_i$  designates the temperature of half peak,  $\Delta T$  is the difference between  $T_p$  and  $T_i$ ,  $\alpha_i$  is the conversion corresponding to the temperature of half peak, and  $(d\alpha/dT)_p$  is the value of a vertical axis corresponding to the temperature of peak.

Next, Equations (2) and (7) can be simplified into:

$$\exp\left(-\frac{E}{RT_i}\right) = \exp\left[-\frac{E}{R_p} \left(1 - \frac{\Delta T}{T_p}\right)\right]. \quad (9)$$

Furthermore, integrating Equations (2), (7) and (9), the result can be displayed as follows:

$$\begin{cases} n = \left[ \Delta T \left(\frac{d\alpha}{dT}\right)_p (1 - \alpha_p)^{-1} + \ln\left(\frac{1 - \alpha_i}{1 - \alpha_p}\right) \right]^{-1} \ln 0.5 \\ E = nRT_p^2 \left(\frac{d\alpha}{dT}\right)_p (1 - \alpha_p)^{-1}. \end{cases} \quad (10)$$

Table 4 presents the feature values and kinetic parameters of samples based on differential weight loss curves. On the ground of these feature values and kinetic parameters, the combustion mechanism is studied using the peak-to-peak method of analysis. The results show that derivative weight loss curves could be described as an overlapping peak of several sub-peaks, employing a combustion kinetics model. The model is useful for researching the combustion process of the mixture of oil shale semi-coke and rice straw.

**Table 4. Feature values and kinetic parameters for samples**

Sample	Sub-peak	T <sub>p</sub> , °C	ΔT, °C	(da/dT) <sub>p</sub> , 1/°C	α <sub>p</sub>	α <sub>i</sub>	n	E, kJ/mol
L1	1	447.54	32.16	0.00260	0.49	0.76	1.17	25.75
	2	488.18	61.75	0.00314	0.50	0.79	1.44	43.58
	3	521.17	72.87	0.00419	0.50	0.80	2.27	99.79
L2	1	447.40	67.64	0.00251	0.50	0.79	1.31	28.39
	2	512.84	73.98	0.00351	0.51	0.80	1.79	65.86
	3	568.55	36.52	0.00143	0.49	0.72	1.39	22.95
L3	1	479.99	71.54	0.00264	0.50	0.77	1.73	43.08
	2	534.68	54.51	0.00262	0.51	0.79	1.25	36.26
	3	564.25	34.81	0.00173	0.52	0.73	1.54	32.35
L4	1	463.94	72.88	0.00213	0.51	0.78	1.43	28.08
	2	531.69	65.18	0.00216	0.50	0.76	1.53	35.60
	3	568.76	30.71	0.00151	0.50	0.74	1.23	21.89

#### 4. Comprehensive evaluation

The kinetic parameters of coal/biomass blends have been worked out by some researchers. Wang et al. [31] and Sahu et al. [32] proposed that activation energies are in the range of from 92 to 114 kJ/mol. However, they only offered activation energies and constant reaction orders for overlapped peaks appearing in different temperature regions during the whole combustion process, not for the sub-peaks separated from the overlapping peak. In this work, each sub-peak corresponds to each component in a particular combustion reaction stage. This means that the whole combustion reaction process consists of the reactions of various sub-peaks. Based on the Gaussian multi-peak fitting and peak-to-peak methods, activation energies and reaction orders of sub-peaks are found. Therefore, compared with the results obtained by Wang et al. [31] and Sahu et al. [32], in this work, the value of activation energies offered from various sub-peaks needs to have a superposition in calculations. The kinetic parameters of semi-coke/biomass blends obtained in this study are more reliable.

In order to analyze the error of calculation, a comprehensive evaluation was made to guarantee the reliability of results. *SS* is defined as a sum of squares of differences between experimental and fitted data to reflect the accuracy of Gaussian multi-peak fitting and peak-to-peak methods. The smaller the value of *SS* is, the higher the accuracy of calculation is. Meanwhile, the equation of *SS* meets the minimum value expressed as follows [33]:

$$SS = \sum_{i=1}^n \omega_i [y_i - f_i(\chi_i, P)]^2, \quad (11)$$

where  $\omega_i$  is the weighted factor,  $n$  is the number of iterations and  $\chi$  is the evaluation function.

Based on Equation (11), the values of  $SS$  and  $R$  are shown in Table 5. For blends L1, L2, L3 and L4, Gaussian multi-peak fitting and peak-to-peak methods displayed the highest correlation coefficients, with values around 0.99900. Besides,  $SS$  can be left unchanged within  $1.0E-7$ . This result appears to be more reliable in view of requirements of calculation.

**Table 5. Correlation coefficient for the Gaussian multi-peak fitting method**

Sample	$R$	$\chi$ (Reduce Chi <sup>2</sup> )	$SS$
L1	0.99964	5.86701E-1	3.20925E-7
L2	0.99987	1.67524E-1	1.18942E-7
L3	0.99968	1.74471E-1	1.00495E-7
L4	0.99889	2.28994E-1	1.2755E-7

## 5. Conclusions

Results of an experimental study on the combustion of Huadian oil shale semi-coke with rice straw are presented. The following conclusions are drawn:

1. The co-combustion of oil shale semi-coke and rice straw is a complicated multistage process and contains many elementary reactions. The combustion reaction parameters, such as ignition temperature, burning temperature, maximum burning rate and peak temperature, are obtained in various stages. The burnout temperature is found to decrease and maximum burning rate increase with increasing rice straw proportion in the blend.
2. A thermogravimetric analysis shows that in the co-combustion of oil shale semi-coke and rice straw the positive interaction between the blend components occurs in the major stage, at 400–600 °C. This stage is merged from the second (400–500 °C) and third (500–600 °C) stages, where the reactions of bimodal components of semi-coke and rice straw overlap. This means that the reaction process of blend components consists of the reactions of various sub-peaks. Based on Gaussian multi-peak fitting and peak-to-peak methods, the reaction orders of various sub-peaks corresponding to samples L1, L2, L3 and L4 are found to be from 1.17 to 2.27. Similarly, activation energies of various sub-peaks are determined to be 21.89–99.79 kJ/mol throughout the analysis of the combustion mechanism. The activation energy value of various sub-peaks tends to balance with increasing rice straw proportion in the blend, which improves the stability of co-combustion.
3. A comprehensive evaluation of various sub-peaks from the DTG curve for the combustion of oil shale semi-coke with rice straw is made. The fitting correlation coefficient is above 0.998 and  $SS$  at the level of E-7. This demonstrates that the results are reliable and can be applied to

analyzing the combustion mechanism of sub-peaks, using the Gaussian multi-peak fitting method.

### Acknowledgements

The authors are grateful for financial support from the Nation Innovative Projects with Co-operation in Terms of Production, Study and Research (The Exploration and Utilization of Oil Shale–OSR–05), and from the Department of Education of Jilin Province, China (2009106).

### REFERENCES

1. Kūlaots, I., Goldfarb, J. L., Suuberg, E. M. Characterization of Chinese, American and Estonian oil shale semicokes and their sportive potential. *Fuel*, 2010, **89**(11), 3300–3306.
2. Dyni, J. R. Geology and resources of some world oil-shale deposits. *Oil Shale*, 2003, **20**(3), 193–252.
3. Brendow, K. Global oil shale issues and perspectives. *Oil Shale*, 2003, **20**(1), 81–92.
4. Ding, A. Z., Fu, J. M., Sheng, G. Y., Liu, P. X., Carpenter, P. J. Effects of oil shale waste disposal on soil and water quality: hydrogeochemical aspects. *Chem. Spec. Bioavailab.*, 2003, **14**, 79–86.
5. Kuusik, R., Martins, A., Pihu, T., Pesur, A., Kaljuvee, T., Prikk, A., Triikkel, A., Arro, H. Fluidized-bed combustion of oil shale retorting solid waste. *Oil Shale*, 2004, **21**(3), 237–248.
6. Wang, Q., Sun, B. Z., Wu, X. H., Bai, J. R., Sun, J. Study on combustion characteristics of mixtures of Huadian oil shale and semicoke. *Oil Shale*, 2007, **24**(2), 135–145.
7. Wang, Q., Wang, H. G., Sun, B. Z., Bai, J. R., Guan, X. H. Interactions between oil shale and its semi-coke during co-combustion. *Fuel*, 2009, **88**(8), 1520–1529.
8. Sun, B. Z., Wang, Q., Shen, P. Y., Liu, H. P., Qin, H., Li, S. H. Experimental investigation on combustion characteristics of oil shale semi-coke and bituminous coal blends. *China Coal Soc.*, 2010, **35**(3), 176–180 (in Chinese).
9. Wang, Q., Zhao, W. Z., Liu, H. P., Jia, C. X., Li, S. H. Interactions and kinetic analysis of oil shale semi-coke with cornstalk during co-combustion. *Appl. Energ.*, 2011, **88**(6), 2080–2087.
10. Yuan, Z. H., Wu, C. Z., Ma, L. L. *Biomass Utilization Principle and Technology*. Chemical Industry Press, Beijing, 2005 (in Chinese).
11. De, S., Assadi, M. Impact of cofiring biomass with coal in power plants – A techno-economic assessment. *Biomass Bioener.*, 2009, **33**(2), 283–293.
12. Yang, T. H., Kai, X. P., Sun, Y., He, Y. G., Li, R. D. The effect of coal sulfur on the behavior of alkali metals during co-firing biomass and coal. *Fuel*, 2011, **90**(7), 2454–2460.

13. Munir, S., Nimmo, W., Gibbs, B. M. The effect of air staged, co-combustion of pulverised coal and biomass blends on NO<sub>x</sub> emissions and combustion efficiency. *Fuel*, 2011, **90**(1), 126–135.
14. Soboleva, E., Ambrus, A., Jarju, O. Estimation of uncertainty of analytical results based on multiple peaks. *J. Chromatogr. A*, 2004, **1029**(1–2), 161–166.
15. Romanenko, S. V., Stromberg, A. G. Classification of mathematical models of peak-shaped analytical signals. *J. Anal. Chem+*, 2000, **55**(11), 1024–1028.
16. Romanenko, S. V., Stromberg, A. G. Modelling of analytical peaks: peaks modifications. *Anal. Chim. Acta*, 2007, **581**(2), 343–354.
17. Wang, G., Li, W., Li, B. Q., Chen, H. K. TG study on pyrolysis of biomass and its three components under syngas. *Fuel*, 2008, **87**(4–5), 552–558.
18. Wang, S. R., Guo, X. J., Wang, K. G., Luo, Z. Y. Influence of the interaction of components on the pyrolysis behavior of biomass. *J. Anal. Appl. Pyrol.*, 2011, **91**(1), 183–189.
19. Huang, Y. Q., Wei, Z. G., Qiu, Z. J., Yin, X. L., Wu, C. Z. Study on structure and pyrolysis behavior of lignin derived from corncob acid hydrolysis residue. *J. Anal. Appl. Pyrol.*, 2012, **93**, 153–159.
20. Li, R., Jin, B. S., Zhong, Z. P., Fu, X. F., Jia, X. R. Mechanism research on rice husk bio-oil combustion based on parallel reaction model. *Proc. CSEE*, 2009, **29**(29), 89–95 (in Chinese).
21. Li, R., Jin, B. S., Zhong, Z. P., Fu, X. F. Research on biomass pyrolysis three-pseudocomponent model by Gaussian multi-peaks fitting. *Acta Energ. Sol. Sin.*, 2010, **31**(7), 806–810 (in Chinese).
22. Ma, W., Wang, S., Cui, J. P., Zhang, S. T., Fan, B. C., He, Y. Z. Thermal decomposition kinetic model of phenolic resin. *Acta Phys. Chim. Sin.*, 2008, **24**(6), 1090–1094.
23. Gil, M. V., Casal, D., Pevida, C., Pis, J. J., Rubiera, F. Thermal behaviour and kinetics of coal/biomass blends during co-combustion. *Bioresource Technol.*, 2010, **101**(14), 5601–5608.
24. Sun, B. Z., Wang, Q., Li, S. H., Wu, X. H., Sun, J., Sun, B. M. Experiment study on combustion performance of oil shale and semi-coke blends. *Proceedings of the CSEE*, 2006, **26**(20), 108–112 (in Chinese).
25. Liu, H. P., Li, W. Y., Zhao, W. Z., Xu, H., Wang, Q. Combustion characteristics of oil shale semi-coke and cornstalk blends. *Journal of Combustion Science and Technology*, 2011, **17**(3), 255–260 (in Chinese).
26. Yu, Q. M., Pang, Y. J., Chen, H. G. Determination of ignition points in coal-combustion tests. *North China Electric Power*, 2001, No. 7, 9–10 (in Chinese).
27. Varol, M., Atımtay, A. T., Bay, B., Olgun, H. Investigation of co-combustion characteristics of low quality lignite coals and biomass with thermogravimetric analysis. *Thermochim. Acta*, 2010, **510**(1–2), 195–201.
28. Özgür, E., Miller, S. F., Miller, B. G., Kök, M. V. Thermal analysis of co-firing of oil shale and biomass fuels. *Oil Shale*, 2012, **29**(2), 190–201.
29. Zhou, J. P. *Proficiency in Origin 7.0*. Beijing University of Aeronautics and Astronautics Press, 2004 (in Chinese).
30. Hu, R. Z., Gao, S. L., Zhao, F. Q., Shi, Q. Z., Zhang, T. L., Zhang, J. J. *Thermal analysis kinetics*. 2nd ed. Science Press, Beijing, 2008 (in Chinese).
31. Wang, C. P., Wang, F. Y., Yang, Q. R., Liang, R. G. Thermogravimetric studies of the behavior of wheat straw with added coal during combustion. *Biomass Bioener.*, 2009, **33**(1), 50–56.

32. Sahu, S. G., Sarkar, P., Chakraborty, N., Adak, A. K. Thermogravimetric assessment of combustion characteristics of blends of a coal with different biomass chars. *Fuel Process. Technol.*, 2010, **91**(3), 369–378.
33. Gregorčič, G., Lightbody, G. Gaussian process approach for modelling of nonlinear systems. *Eng. Appl. Artif. Intel.*, 2009, **22**(4–5), 522–533.

*Presented by V. Oja*

Received May 9, 2012